Bound soliton pairs in photonic crystal fiber

A. Podlipensky, P. Szarniak, N. Y. Joly*, C. G. Poulton and P. St.J. Russell

Max-Planck Research Group (IOIP), University of Erlangen-Nuremberg
Guenther-Scharowsky Str. 1/Bau 24, 91058 Erlangen, Germany
**current address: Laboratoire de Physique des Lasers, Atomes et Molécules Université des Sciences et Technologies de Lille, 59655 Villeneuve d'Ascq Cedex, France*
apodlipensky@optik.uni-erlangen.de

Abstract: We demonstrate experimentally the formation and stable propagation of bound soliton pairs in a highly nonlinear photonic crystal fiber. The bound pairs occur at a particular power as the consequence of high-order soliton fission. They propagate over long distances with constant inter-soliton frequency and time separation. During propagation, the soliton self-frequency shift causes the central frequency of the pairs to move towards longer wavelength. The formation and characteristics of the bound soliton pairs are confirmed numerically. We believe this to be the first experimental observation of such bound soliton pairs.

OCIS codes: (060.5530) Pulse propagation and solitons; (060.4370) Nonlinear optics, fibers; (060.7140) Ultrafast processes in fibers.

References and links

1. A. Hasegawa and F. Tappert, "Transmission of stationary nonlinear optical pulses in dispersive dielectric fibers. I. Anomalous dispersion," Appl. Phys. Lett. **12**, 142-144 (1973).
2. L. F. Mollenauer, R. H. Stolen and J. P. Gordon, "Experimental observation of picosecond pulse narrowing and solitons in optical fibers," Phys. Rev. Lett. **45**, 1095-1098 (1980).
3. A. Hasegawa and M. Matsumoto, *Optical Solitons in Fibers*, (Springer Verlag, Berlin, Heidelberg, 2003).
4. Y. S. Kivshar and G. P. Agrawal, *Optical Solitons*, (Academic Press, San Diego, 2003).
5. J. P. Gordon, "Interaction forces among solitons in optical fibers," Opt. Lett. **8**, 596-598 (1983).
6. F. M. Mitschke and L. F. Mollenauer, "Experimental observation of interaction forces between solitons in optical fibers," Opt. Lett. **12**, 355-357 (1987).
7. Y. Kodama and A. Hasegawa, "Effects of initial overlap on the propagation of optical solitons at different wavelengths," Opt. Lett. **16**, 208-210 (1991).
8. S. Chi and S. Wen, "Raman cross talk of soliton collision in a lossless fiber," Opt. Lett. **14,** 1216-1218 (1989).
9. B. J. Hong and C. C. Yang, "Interaction between femtosecond solitons in optical fibers," J. Opt. Soc. Am. B **8**, 1114-1121 (1991).
10. E. Feigenbaum and M. Orenstein, "Colored soliton interactions: particle-like and beyond," Opt. Exp. **12**, 2193-2206 (2005).
11. E. Feigenbaum and M. Orenstein, "Coherent interaction of colored solitons via parametric processes: modified perturbation analysis," J. Opt. Soc. Am. B **22**, 1414-1423 (2005).
12. Y. Kodama and A. Hasegawa, "Nonlinear pulse propagation in a monomode dielectric guide," IEEE J. Quantum Electron. **23**, 510-524 (1987).
13. F. M. Mitschke, L. F. Mollenauer, "Discovery of the soliton self-frequency shift," Opt. Lett. **11**, 659-661 (1986)
14. J. P. Gordon, "Theory of the soliton self-frequency shift," Opt. Lett. **11**, 662-664 (1986).
15. J. Herrmann, A. Nazarkin**,** "Soliton self-frequency shift for pulses with a duration less than the period of molecular oscillations," Opt. Lett. **19**, 2065-2067 (1994).
16. K. Tai, A. Hasegawa and N. Bekki, "Fission of optical solitons induced by stimulated Raman effect," Opt. Lett. **13**, 392-394 (1988).
17. A. B. Grudinin, E. M. Dianov, D. V. Korobkin, A. M. Prokhorov, V. N. Serkin and D. V. Khaidarov, "Decay of femtosecond pulses in single-mode optical-fibers," JETP Lett. **46**, 221-225 (1987).
18. P. Beaud, W. Hodel, B. Zysset and H. P. Weber, "Ultrashort pulse propagation, pulse breakup, and fundamental soliton formation in a single-mode optical fiber," IEEE J. Quantum Electron **QE-23**, 1938-1946 (1987).
19. N. Akhmediev, W. Krolikowski and A. J. Lowery, "Influence of the Raman-effect on solitons in optical fibers," Opt. Commun. **131**, 260-266 (1996).
20. J. C. Knight, T. A. Birks, P. St.J. Russell and D. M. Atkin, "All-silica single-mode fiber with photonic crystal cladding," Opt. Lett. **21**, 1547-1549 (1996).

#77556 - $15.00 USD Received 29 November 2006; revised 10 January 2007; accepted 13 January 2007

21. J. C. Knight, T. A. Birks, P. St.J. Russell and D. M. Atkin, "All-silica single-mode fiber with photonic crystal cladding: errata," Opt. Lett. **22**, 484-485 (1997).
22. P. St.J. Russell, "Photonic crystal fibers," Science **299**, 358-362 (2003).
23. J.M. Dudley, G. Genty, S. Coen, "Supercontinuum generation in photonic crystal fiber," Rev. Mod. Phys. **78**, 1135-1184 (2006).
24. D. V. Skryabin, F. Luan, J. C. Knight and P. St.J. Russell, "Soliton self-frequency shift cancellation in photonic crystal fibers," Science **301**, 1705-1708 (2003).
25. J. Herrmann, U. Griebner, N. Zhavoronkov, A. Husakou, D. Nickel, J. C. Knight, W. J. Wadsworth, P. St.J. Russell and G. Korn, "Experimental evidence for supercontinuum generation by fission of higher-order solitons in photonic fibers," Phys. Rev. Lett. **88**, 173901 (2002).
26. A. Efimov, A. V. Yulin, D. V. Skryabin, J. C. Knight, N. Joly, F. G. Omenetto, A. J. Taylor and P. St.J. Russell, "Interaction of an optical soliton with a dispersive wave," Phys. Rev. Lett. **95**, 213902 (2005).
27. F. Luan, D. V. Skryabin, A. V. Yulin and J. C. Knight, "Energy exchange between colliding solitons in photonic crystal fibers," Opt. Express **14**, 9844-9853 (2006).
28. A. Zheltikov, "Nanoscale nonlinear optics in photonic crystal fibers," J. Opt. A **8**, S47-S72 (2006).
29. M. Bredol, D. Leers, L. Bosselaar and M. Hutjens, "Improved model for OH absorption in optical fibers," J. Lightwave Technol. **8**, 1536-1540 (1990).
30. R. Trebino, *Frequency-Resolved Optical Gaiting: the measurement of ultrashort laser pulses*, (Kluwer Academic Publishers, 2000).
31. G. P. Agrawal, *Nonlinear Fiber Optics* (Academic Press, San Diego, 2001), 3rd ed.
32. K. J. Blow and D. Wood, "Theoretical description of transient stimulated Raman scattering in optical fibers," IEEE J. Quantum Electron. **25**, 2665-2673 (1989).
33. Q. Lin and G. P. Agrawal, "Raman response function for silica fibers," Opt. Lett. 31, 3086-3088 (2006).

1. Introduction

The propagation of solitons in optical fibers has been much studied over the last three decades [1-4]. Potential applications in optical telecommunications and nonlinear optical switching have created strong interest in the different nonlinear effects that arise between interacting solitons [5-11]. It has been shown that the forces acting between two adjacent ps solitons are driven mostly by the Kerr nonlinearity and depend on the initial time separation and relative phase – the forces decrease exponentially with time delay. In-phase solitons show attractive forces, while a relative phase of π causes soliton repulsion [6]. The interaction of solitons with different optical frequencies is more complicated and depends on the frequency separation, time delay and initial pulse energy [7]. For fs solitons, higher-order dispersion and Raman scattering strongly affect the propagation. The solitons shift towards longer wavelengths as a result of the Raman-induced soliton self-frequency shift (SSFS) [12-14]. The magnitude of the SSFS ω_R can be determined by the equation $d\omega_R/dz \propto |\beta_2(z)|/T_0^4$ [14], where z is the propagation distance, T_0 is the soliton width and $\beta_2(z)$ is the GVD parameter. However, this expression is valid only when the pulse duration is longer than the period of molecular oscillations in silica glass, or about 75 fs [15]. For shorter pulses the SSFS depends inversely on the soliton width T_0. At the same time, higher-order dispersion and Raman gain cause fission of higher order solitons, which break up into several red-shifting fundamental solitons [16-18]. Colliding solitons can also exchange energy through inter-pulse Raman scattering, which plays, at the same time, a mainly repulsive role in the collision. However, the energy transfer rate between the two adjacent solitons is also dependent on their temporal and spectral spacing as well as their relative intensities [8,9]. Thus, under particular circumstances a pair of solitons can form a bound state, which can propagate over long distances without changes in its profile, even in the presence of the Raman effect [19].

The development of highly nonlinear photonic crystal fibres (PCFs) [20-22], where the mode fields are tightly confined to an extremely small core and the dispersion can be tailored so as to allow convenient generation and study of solitons, has enabled researchers to investigate soliton interactions in many different nonlinear regimes [23-28].

In this paper we demonstrate experimentally, for the first time to our knowledge, the formation of bound pairs of solitons in highly nonlinear PCF. The pairs are generated by break-up of higher order solitons, and each member of each pair experiences a different SSFS, leading to a decrease in the temporal and spectral spacing between the soliton pair as the input

#77556 - $15.00 USD Received 29 November 2006; revised 10 January 2007; accepted 13 January 2007

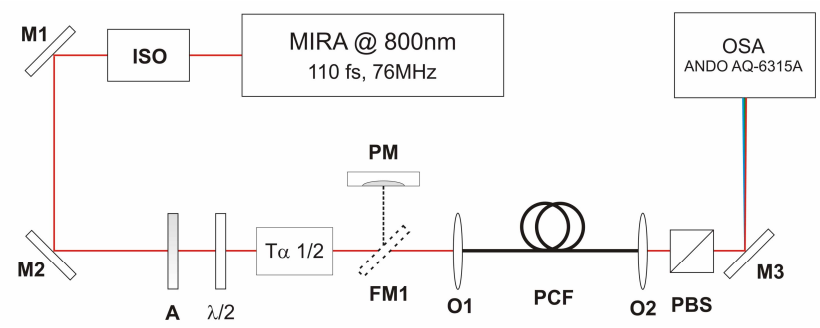

Fig. 1. Experimental setup: ISO, optical isolator; M1,2,3 mirrors; A, attenuator; λ/2, half-waveplate; Tα ½, telescope; FM1, flip mirror; PM, power meter; O1,2, objectives; PCF, highly nonlinear photonic crystal fiber; PBS, polarization beam splitter; OSA, optical spectrum analyzer.

power increases. This eventually results in the formation of a trapped pair of solitons when the spacing becomes sufficiently small. We observe that the trapped soliton pair continues to propagate along the PCF with constant frequency spacing and time delay, while the central frequency of the pair shifts to lower frequencies due to the SSFS. We also present the results of numerical calculations that confirm the experimental observations.

2. Experimental results

The experimental setup is shown in Fig. 1. The pulsed laser source was a commercial mode-locked Ti:sapphire laser (Coherent Mira 900D) operating at 800 nm with a repetition rate of 76 MHz, an average power of 532 mW, pulse energies of up to 7nJ and FWHM pulse durations of 110 fs. The peak power for the laser pulses (assuming a sech^2 pulse shape) was ~56 kW. The laser light was coupled into the PCF using a 60x focusing objective, with launch efficiencies of up to 45%. In order to maximize the launch efficiency, a telescope was placed before the coupling objective to adjust the laser beam diameter to the aperture of the focusing lens. The linear laser polarization at the input was aligned parallel to the birefringent fiber axes using a half-wave plate. For measurements of the polarized spectra at the fiber output, a Glan polarization prism was placed at the end of the fiber after the collimating objective. The spectra were measured using an optical spectrum analyser. A graded reflecting filter was used to control the input power into the fibre.

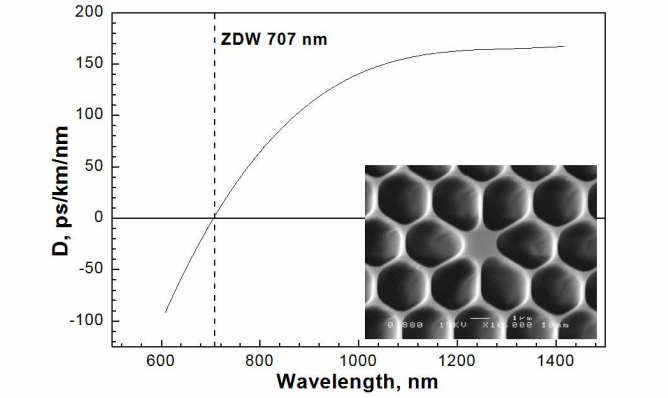

Fig. 2. Dispersion of the PCF used in experiments. Inset: scanning electron micrograph of the fiber cross-section.

#77556 - $15.00 USD Received 29 November 2006; revised 10 January 2007; accepted 13 January 2007

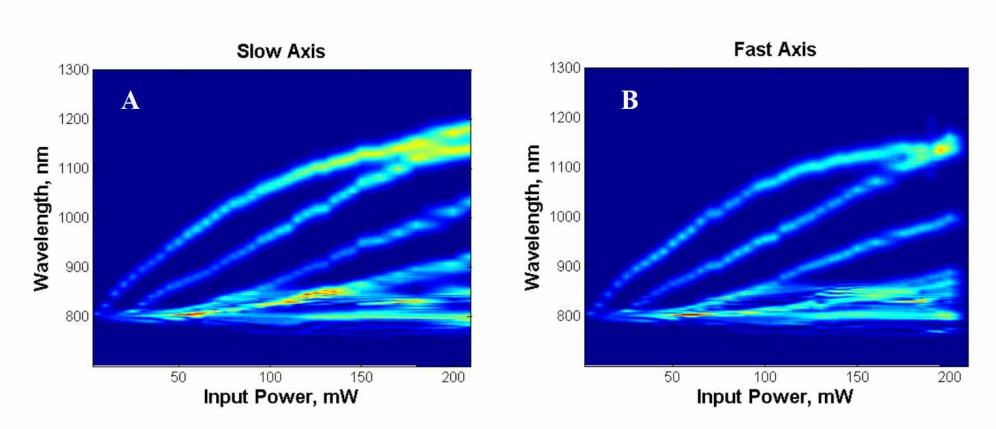

Fig. 3. Spectral evolution with increasing average power. The fiber length is 44 cm and light was launched and detected with polarization parallel to the slow (A) and fast (B) axis of the fiber.

In the experiments we used a silica glass PCF with the group velocity dispersion (GVD) profile shown in Fig. 2. The GVD was measured experimentally using white-light interferometry. The zero dispersion wavelength occurs at 707 nm and the pump laser wavelength lies within the region of anomalous dispersion. The diameter of the fiber core (~1.5 μm), the pitch (~2.75), diameter of air holes (~2.7 μm) and width of the silica webs between holes (~50 nm) were estimated from a scanning electron micrograph of the cross-section (see the inset in Fig. 2). Assuming a dispersion D = 64 ps/km/nm ($\beta_2 = -21.8$ ps^2/km) at 800 nm, the dispersion length $L_D = T_0^2 / |\beta_2|$ was calculated to be 17.9 cm, where the pulse width T_0 is equal to the FWHM pulse duration divided by 1.763. At the same time, the nonlinear length $L_{NL} = 1/\gamma P_0$ (γ=0.0978 W^{-1}m^{-1} and P_0 is the peak pulse power) is as short as 0.4 mm for maximum launched laser power assuming a coupling efficiency of 45% (P_0=25.2 kW). Therefore the maximum soliton order of the input pulse (determined by $N = \sqrt{L_D / L_{NL}}$) is $N \approx 21$. Moreover, despite the apparently round core and symmetrical structure, the PCF displayed weak birefringence, caused perhaps by residual stress.

The Fig. 3 shows the polarized spectra at the output of a fiber of length 44 cm, measured as a function of input power. For the data presented in Fig. 3(A) the excitation and measurement was performed with polarization parallel to the slow axis, while for the spectra in the Fig. 3(B) the polarization of the input pulses and polarizer at the output of the fiber were aligned parallel to the fast axis. Increasing the input power leads to the generation of several spectral bands, red-shifted from the 800 nm pump, and associated with solitons caused by higher order soliton fission and subsequent SSFS to longer wavelengths [23]. The frequency shift of the solitons is a nonlinear function of power; as a result the 1st and 2nd soliton curves approach each other until the frequency spacing between them reaches a minimum at 180 mW (Fig. 3(A)). Small changes in power at this point cause spectral instabilities and soliton overlap. At still higher power the solitons separate spectrally once again. A similar joining of spectral bands is also observed for the 3rd and 4th solitons, which shift together towards longer wavelength until at 100 mW they split into two distinct solitons. In general, the spectral behaviour of solitons excited with polarization parallel to the fast axis (Fig. 3(B)) is very similar to excitation parallel to the slow axis (Fig. 3(A)). However, in the former case the spectral overlap of the solitons (top right-hand corner of Fig. 3(B)) is accompanied by polarization switching between fast and slow axes. Apparently, interaction between different polarization components causes subtle but important differences in the measured spectra. To avoid additional polarization effects we consider here only excitation of the slow axis.

#77556 - $15.00 USD Received 29 November 2006; revised 10 January 2007; accepted 13 January 2007

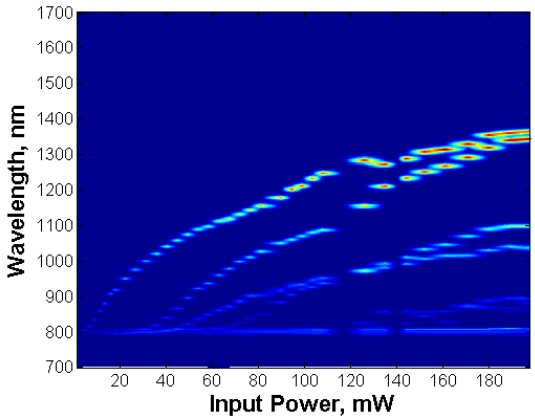

Fig. 4. Spectral evolution with increasing power. Fiber length was 15 m. Excitation and detection parallel to the slow axis.

Figure 4 shows the dependence of the spectra at the output from the 15 m fiber as a function of the input power. As can be seen, the behaviour of the solitons with increasing power is quite similar to that shown in Fig. 3 for the 44 cm fiber: the spectral bands of the 1st and 2nd solitons shift towards long wavelength (via SSFS) and approach each other until the frequency spacing between them reaches a minimum at approximately 180 mW. At the same time, the 3rd and 4th solitons overlap spectrally in the power range between 100 and 130 mW, which is in quite good agreement with the data shown in Fig. 3. The input power of about 180 mW corresponds in our experiment to an 8.5 kW peak pulse power in the fiber and the maximum soliton number for this power is N=12.2. Moreover, the power dependences measured during cut-back experiments always indicated overlapping of the spectral bands of the 1st and 2nd solitons close to 180 mW of input power for all fiber lengths between 44 cm and 15 m. This indicates that for the input power of 180 mW the fission of higher order solitons results in a pair of solitons, which propagate in the fiber with closely spaced frequencies. In order to prove this conclusively we studied the spectra as a function of the fiber length.

The evolution of the spectrum with propagation distance is shown in Fig. 5. The input power (kept constant throughout) corresponds to the case of minimum inter-soliton spectral spacing near to 180 mW. As can be seen in Fig. 5(A), laser pulses at 800 nm launched into the

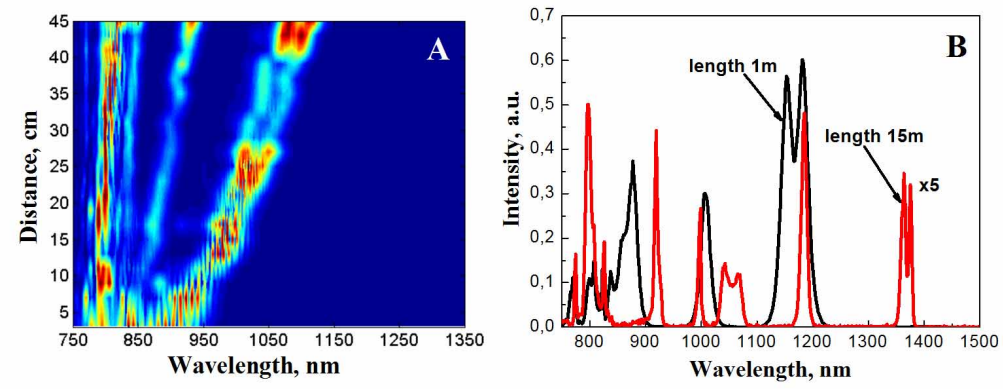

Fig. 5. A-Evolution of the spectra with length. B - the spectra for the 1m (black line) and for the 15m (red line) fiber. The input power of ~180 mW (constant throughout) corresponded to the minimum spectral spacing between the solitons. Both excitation and measurement were performed parallel to the slow axis.

#77556 - $15.00 USD Received 29 November 2006; revised 10 January 2007; accepted 13 January 2007

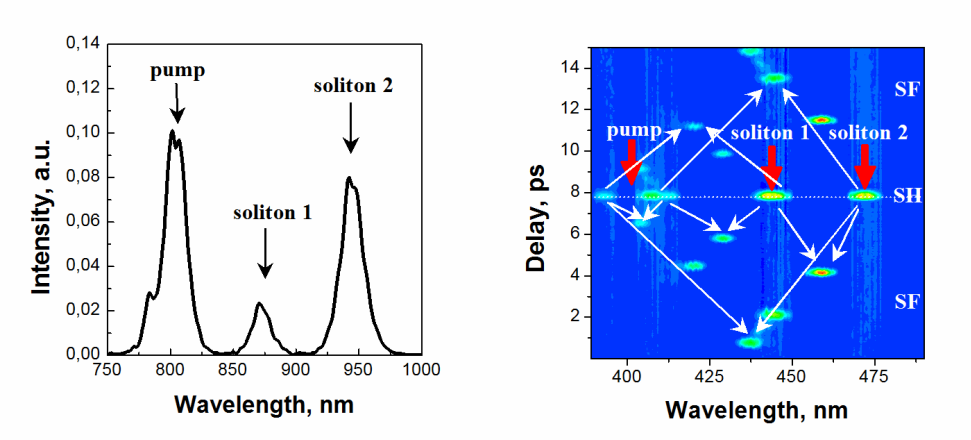

Fig. 6. A typical spectrum at the output of the fiber and corresponding FROG spectrograph. The wavelength scale in spectrogram is not recalculated and presents the spectra of the output signal due to the frequency-doubling in the FROG. The white arrows indicate spectral components responsible for the sum frequency peaks.

fiber broaden spectrally and the center of the spectrum shifts to 860 nm within the first 5 cm of propagation (i.e., about one quarter of the dispersion length $L_D \approx 17.9$ cm), indicating the effects of SPM and intra-pulse Raman scattering. Subsequent pulse propagation along the fiber results in the formation of an additional pulse at 930 nm, which transforms later into a pair of adjacent solitons. The mean frequency of the soliton pair shifts steadily towards longer wavelengths due to the SSFS. At the same time, the spectral spacing between them remains almost constant even after 15 m (Fig. 5(B)). On the other hand, the fiber attenuation causes energy loss, leading to spectral narrowing and temporal broadening of the solitons as they propagate (Fig. 5(B)). The losses are related to the strong OH absorption band at 1.4 μm [29]. This in turn restricts the SSFS and explains the strong narrowing and damping of the solitons near 1.4 μm (Fig. 5(B)). We conclude that losses and changes in the soliton parameters cause the observed small decrease of inter-soliton spectral spacing in 15 m fiber, as compared to the spectral spacing in the 1 m fiber (Fig. 5(B)).

Using second-harmonic frequency-resolved optical gating (SH FROG) [30], it is possible to check that the spectrally overlapping solitons co-propagate in time. The time delay between two solitons of different color travelling at different group velocities can be estimated from the sum-frequency (SF) peaks occurring between the center frequencies of the two solitons. In Fig. 6(A) a typical output spectrum is shown, with pump light at 800 nm and two red shifted solitons at 870 nm and 943 nm. The corresponding SHG FROG spectrograph can be seen in Fig. 6(B). The second harmonic (SH) signals from each spectral component appear in the middle of the spectrograph (shown as dashed line). All spots above and below the line are the result of SF generation between the pump laser pulse and the two solitons. The corresponding SF components are shown by arrows. The delay between two different pulses can be estimated from the time between SF components and SH signals of corresponding pulses (Fig. 6(A)).

The FROG spectrographs of the soliton pair, measured for different lengths of fiber, are presented in Figs. 7 and 8 as a function of the input power. In Fig. 7(A) a soliton pair appears in 70 cm fiber. The spectral spacing between the solitons (~50 nm) is defined by the input power and corresponds in Fig. 3 to the point close to soliton overlap (at a power of ~180 mW). The delay between the solitons is ~3 ps. With increasing power the frequencies of the solitons approach each other (Fig. 7(B-D)), which agrees with the spectra presented in Fig. 3. At the same time, the delay between the SF component and SH signal from the soliton pair decreases, indicating a reduction in the delay between the solitons. If the frequency shift is a minimum, the delay is ~400 fs (Fig. 7(D)). A further increase in the power leads to the collision of the solitons in time and frequency, resulting in strong temporal beats in the SH

#77556 - $15.00 USD Received 29 November 2006; revised 10 January 2007; accepted 13 January 2007

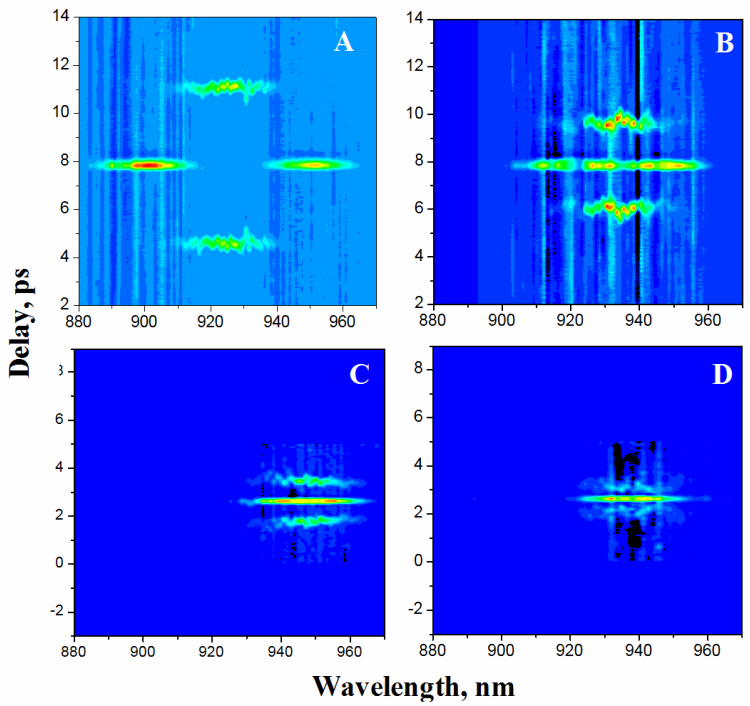

Fig. 7. FROG spectrographs of the soliton pair in 70 cm fiber for different power levels. The input power is increasing stepwise from image A to image D. The image D corresponds to input power of 180 mW in Fig. 3.

signal – the signature of a strong nonlinear interaction. A similar FROG trace was measured for a fiber of length 150 cm (Fig. 8). If the spectral spacing between solitons is ~40 nm (Fig. 8(A)) the solitons co-propagate with a delay ~4 ps. With increasing power, the solitons approach each other in frequency and time. At the moment when the solitons have minimum spectral spacing at 180 mW of launched power, the time delay between them is reduced to 400 fs (Fig. 8(C)), just as in Fig. 7(D). Further increase in power leads to strong instabilities in the FROG signal, indicating the presence of strong nonlinear interactions between the solitons during the collision. The same behavior has also been observed in 15 m of fiber, where however the soliton pair appears close to 1400 nm, i.e., at the detection limit of the FROG device. Thus, the SH and SF signals were very weak and noisy, but the general behavior was the same as for shorter lengths of fiber.

These results suggest that once the correct launch conditions (pulse energy and duration)

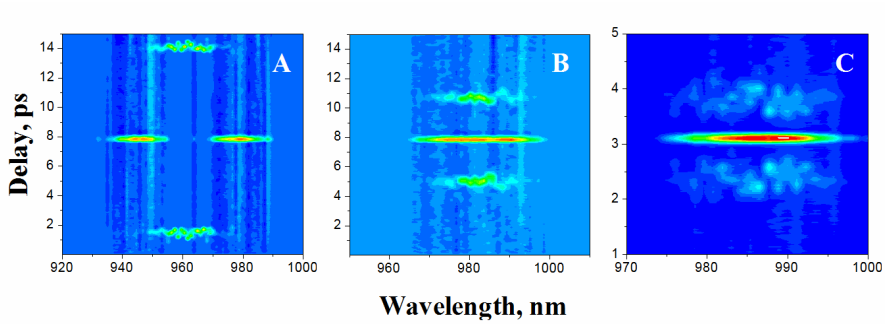

Fig. 8. FROG spectrographs of the soliton pair in 150 cm fiber for different power levels. The input power is increasing stepwise from image A to image C. The image C corresponds to an input power of 180 mW in Fig. 3.

#77556 - $15.00 USD Received 29 November 2006; revised 10 January 2007; accepted 13 January 2007

are met, a bound soliton pair forms almost immediately and propagates over long distances along the fiber while preserving its inter-soliton spectral and temporal spacing.

3. Theoretical results and discussion

In order to better understand the observed behaviour we have solved the generalized nonlinear Schrödinger equation (GNLSE), which governs the evolution of ultrashort pulses in optical fibers [31, 32]:

$$\frac{\partial A(z,\tau)}{\partial z}=\sum_{n\geq 2}^{\infty}\frac{i^{n+1}\beta_n}{n!}\frac{\partial^n A(z,\tau)}{\partial \tau^n}-\frac{\alpha}{2}A(z,\tau)+i\gamma\left(1+\frac{i}{\omega_0}\frac{\partial}{\partial\tau}\right)\left(A(z,\tau)\int_{-\infty}^{\infty}R(t')\left|A(z,\tau-t')\right|^2dt'\right) \quad (1)$$

where $A(z,\tau)$ is the slowly varying envelope of the pulse, τ is time in a reference frame propagating with the group velocity v_g of the input pulse, $\beta_n=\partial^n\beta/\partial\omega_o^n$ represents the coefficients in the Taylor expansion of the propagation constant expanded around the carrier frequency ω_o, α is power attenuation, γ is the nonlinear parameter of the fiber and $R(t)$ is the Raman response function defined by:

$$R(t)=(1-f_R)\delta(t)+f_R\left(q_a h_a(t)+q_b h_b(t)\right) \quad (2)$$

where

$$h_a(t)=\frac{\tau_1^2+\tau_2^2}{\tau_1\tau_2^2}\exp(-t/\tau_2)\sin(t/\tau_1),\quad h_b(t)=\frac{2\tau_b-t}{\tau_b^2}\exp(-t/\tau_b). \quad (3)$$

Expression (2) takes into account both the instantaneous electronic and the delayed molecular response of fused silica, and following a recent paper includes both isotropic and anisotropic Raman responses [33].The characteristic times are τ_1 = 12.2 fs, τ_2 = 32 fs and τ_b = 96 fs and the weighting factors are $f_R=0.245$, $q_a=0.79$ and $q_b=0.21$ [32,33].

The GNLSE was solved using the symmetrized split-step Fourier transform method (SSFM) [31]. Since in all the experiments reported here the light was polarised parallel to the slow axis of the fiber, the GNLSE in its full vector form was not necessary and a purely scalar approach was used.

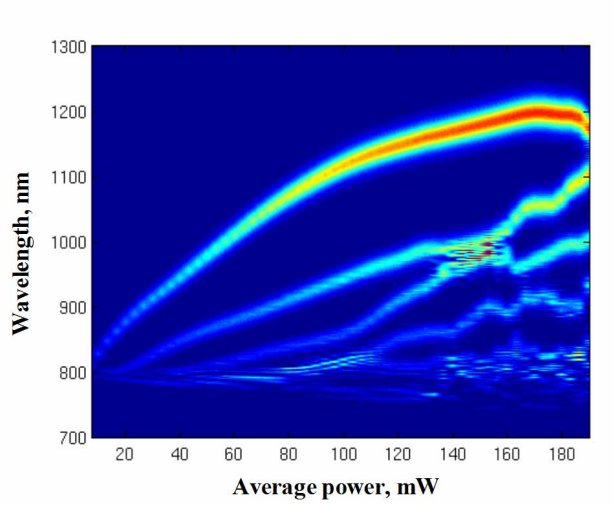

Fig. 9. Numerical simulation of spectral evolution with increasing input average power. The laser launch efficiency is taken to be 30%. Fiber length is 44 cm.

#77556 - $15.00 USD Received 29 November 2006; revised 10 January 2007; accepted 13 January 2007

In estimating the nonlinear coefficient $\gamma = n_2\omega_o / cA_{eff}$, the effective area of the fundamental mode was approximated by the area of solid glass core. Taking the nonlinear refractive index of silica to be $n_2 = 2.2\times10^{-20}$ m^2/W, the calculated nonlinear coefficient is $\gamma = 0.0978$ W^{-1}m^{-1} at a pump wavelength of λ_p = 800 nm. The dispersion coefficients were calculated by fitting to the experimental GVD curve (Fig. 2) using a fifth order Taylor expansion. The launched pulse was taken to have a hyperbolic-secant profile and to be chirp-free, which approximately matches the pulse characteristics of the Ti:sapphire laser used in the experiments.

The numerically calculated spectra are shown as a function of average power in Fig. 9. The power range corresponds to the experimental data, taking into account launch efficiency into the fiber. The fission of the pump pulse into several fundamental solitons, which shift to longer wavelengths with increasing power, is clearly apparent. For power levels up to 30 mW the calculated spectra closely follow the experimental data (Fig. 3). Beyond this point, however, the numerical results show overlap of the 2nd and 3rd solitons, rather than the 1st and 2nd as in the experiment. The discrepancy could be due to OH-related losses at 1.4 μm, which are not considered in our model. Nevertheless, soliton pair formation in the numerical model

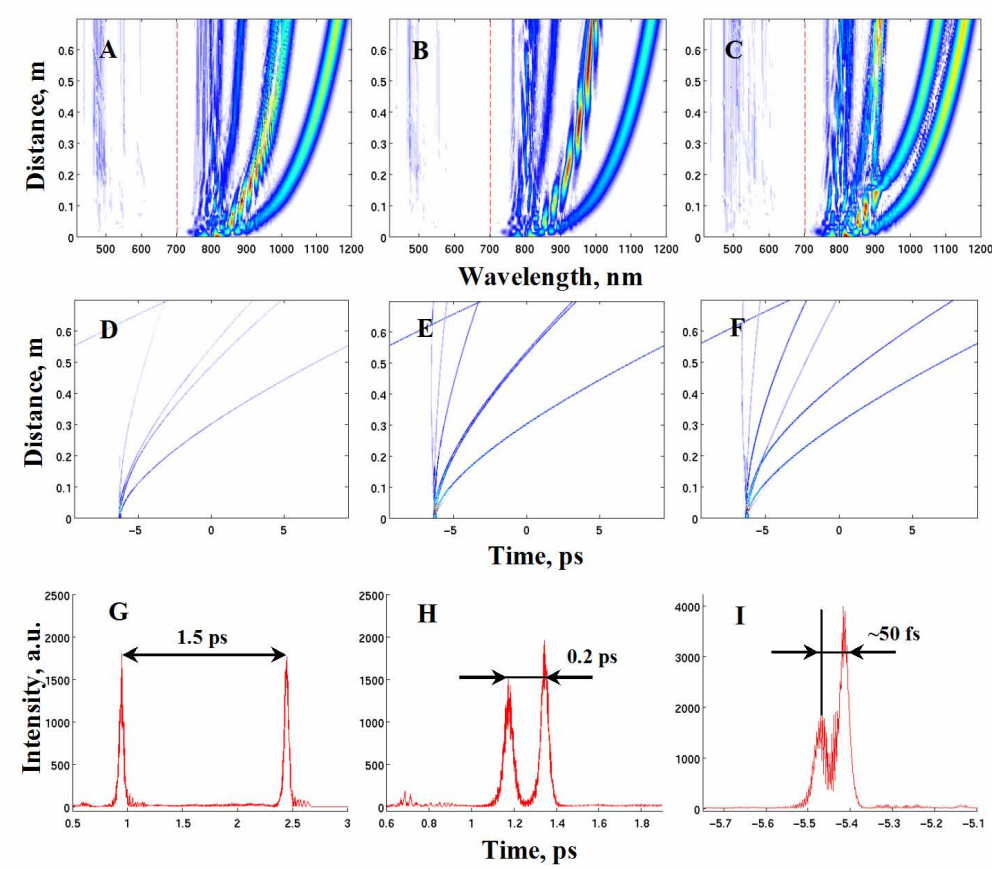

Fig. 10. Numerical modelling of the spectral (A,B,C) and temporal evolution (D,E,F) of launched laser pulses in 70 cm PCF for three different power levels (below, at, and above bound state formation; the input power increases stepwise from A to C). G & H: soliton splitting (G) and bound pair formation (H) after 60 cm of propagation. I: the solitons before collision at the distance of 16 cm.

#77556 - $15.00 USD Received 29 November 2006; revised 10 January 2007; accepted 13 January 2007

and the experiment are qualitatively similar. We can make use of the effect to study the spectral and temporal behaviour of a soliton pair as a function of fiber length. The results of numerical simulations are presented in Fig. 10 for three different power levels close to 150 mW, corresponding to the spectral overlap of the 2nd and 3rd solitons (Fig. 9). The stable co-propagation of the two solitons occurs over a narrow range of power – only a few mW. Figs. 10(A) and 10(D) show the spectral and temporal evolution of solitons in the fiber for powers lower than those needed for the formation of a bound soliton pair. Higher order soliton fission in the first few cm results in break-up of the pump pulse into several fundamental solitons, together with creation of a bound soliton pair (the 2nd and 3rd). As can be seen in Fig. 10(A), the solitons propagate over 70 cm, with their spectra overlapping. However, the time delay between them increases with distance (Fig. 10(D)), reaching ~1.5 ps after 60 cm of propagation (Fig. 10(G)). A small further increase in power results in a decrease in the time delay at the output, and the solitons co-propagate over 70 cm (Fig. 10(E)) with a constant ~200 fs time separation (Fig. 10(H)). At the same time, the spectrum consists of two bands which oscillate in strength as the length of fiber increases (Fig. 10(B)). The spectral spacing between the bands remains constant, however, and is clearly related to the time delay between the solitons.

Next the average power is set to a value above that required for spectral overlap of the solitons (Fig. 9). Over the first 18 cm, the spectral and temporal behavior (Figs. 10(C) and 10(F)) is very similar to the two last cases. However, close to 18 cm the solitons collide and Raman scattering causes strong inter-pulse energy transfer (Fig. 10(I)). After collision the solitons split spectrally (Fig. 10(C)), the soliton with lower energy propagates with almost constant frequency while the stronger one shows a more pronounced SSFS. Temporal separation of the solitons after collision is also apparent (Fig. 10(F)), and follows from the spectral splitting.

In summary, numerical simulations and experimental measurements show very similar behaviour of the bound soliton pairs propagating along PCF. The bound soliton pairs are generated within a narrow power range (177-183 mW), and are a product of the fission of higher order solitons. The numerical model used did not include spectrally-dependent fibre losses, which in the experiment cause spectral narrowing (temporal broadening) of solitons propagating long distances in the PCF. It is clear that broadening of the interacting solitons will decrease the strength of the Raman effect, which itself causes soliton repulsion. In presence of the losses, therefore, the bound soliton pair is expected to be more stable with propagation distance.

4. Conclusions

The fission of higher order solitons in PCF creates a series of fundamental solitons which propagate with differing amounts of SSFS. As a result it is possible to explore the interactions between pairs of solitons without the need to launch independent solitons into the fibre. In the experiments, the temporal and spectral spacing between a soliton pair can be adjusted by changing the input power level. When the frequency spacing and temporal separation are small enough, the solitons can form a quasi-stable pair which continues to propagate along the PCF with constant frequency spacing and time delay, or collide demonstrating strong energy exchange resulting in spectral splitting and increasing time delay. Once formed, bound soliton pairs propagate over long distances in PCF without noticeable change in their temporal and spectral spacing. Numerical solutions of the GNLSE confirm these conclusions.

#77556 - $15.00 USD Received 29 November 2006; revised 10 January 2007; accepted 13 January 2007